

Improved adhesive strength and toughness of polyvinyl acetate glue on addition of small quantities of graphene

Umar Khan<sup>1</sup>, Peter May<sup>1</sup>, Harshit Porwal<sup>1</sup>, Khalid Nawaz<sup>2</sup> and Jonathan N Coleman<sup>1\*</sup>

<sup>1</sup>*School of Physics and CRANN, Trinity College Dublin, Dublin 2, Ireland*

<sup>2</sup>*Department of Chemical Engineering, School of Chemical and Materials Engineering (SCME), National University of Sciences and Technology, H-12, Islamabad, Pakistan*

[\\*colemaj@tcd.ie](mailto:colemaj@tcd.ie)

**ABSTRACT:** We have prepared composites of polyvinyl acetate (PVAc) reinforced with solution exfoliated graphene. We observe a 50% increase in stiffness and a 100% increase in tensile strength on addition of 0.1vol% graphene compared to the pristine polymer. As PVAc is commonly used commercially as a glue, we have tested such composites as adhesives. The adhesive strength and toughness of the composites were up to 4 and 7 times higher, respectively, than the pristine polymer.

**Keywords:** graphene, composite, adhesive, tensile, shear, strength

## 1. Introduction

Adhesives play a critical role of modern manufacturing, and are essential in a wide range of areas from packaging to electronics<sup>1</sup> to aerospace technology<sup>2,3</sup>. While they come in many forms, possibly the simplest are synthetic thermoplastic adhesives. Essentially, these are high concentration polymer solutions which can be spread on the surfaces to be bonded. After the surfaces are brought into contact the solvent slowly evaporates to give a solid polymer which forms an effective bond.

In general, adhesives can fail cohesively or adhesively, that is within the bulk of the adhesive or at the adhesive-surface interface. Many synthetic thermoplastic adhesives form relatively strong interfacial bonds. In addition, when a porous material such as wood is bonded, the adhesive can permeate into the pores, resulting in mechanical interlocking and an increase in the bonded area.<sup>4</sup> This means that the limitations of synthetic thermoplastic adhesives can sometimes be associated with the mechanical properties of the polymer. Amorphous polymers tend to have limited mechanical strengths which are generally below ~50 MPa.<sup>5</sup> In addition, many of the thermoplastics commonly used as adhesives have a glass transition temperature which is close to room temperature<sup>6</sup> resulting in limited thermal stability of the bond.<sup>4</sup> It is common practise to modify the properties of the adhesive by the addition of additives. While such additives are usually included to alter the adhesive properties,<sup>7-9</sup> some researchers have used additives to improve the mechanical properties of the adhesive.<sup>10, 11</sup> In addition, it is worth noting that in the last few years a small number of researchers have begun to explore using nano-materials as additives in adhesives<sup>9-12</sup>

One of the most commonly used thermoplastic adhesives is polyvinyl acetate (PVAc).<sup>4, 10, 13, 14</sup> We note that this material is not to be confused with polyvinyl alcohol (PVA), a polymer that has been much studied as a nano-composite matrix.<sup>15, 16</sup> Generally found as a water-based emulsion, PVAc is most often used as an adhesive for porous materials such as wood and paper. As such, it generally forms a strong adhesive bond and so the adhesive strength tends to be limited by the mechanical properties of the polymer. A number of papers have described reinforcement<sup>17</sup> of PVAc with nano-materials such as carbon nanotubes,<sup>18</sup> cellulose nanofibers<sup>19</sup> or nanoclays<sup>20</sup>. Adhesives based on PVAc loaded with small quantities of nanoclays have even exhibited small but significant increases in adhesive strength.<sup>10</sup>

However, the adhesives studied all display some negative aspects. For example, carbon nanotubes, while very promising as a filler due to their extremely high strength and stiffness<sup>17</sup> are ultimately impractical due to their high cost. At the other extreme, nanoclays are extremely cheap but do not have the superlative mechanical properties displayed by nanotubes.<sup>21, 22</sup> However, recently a new nanomaterial has become available which combines the high strength of carbon nanotubes with the low cost of clays. Graphene is a 2-dimensional sheet of sp<sup>2</sup> bonded carbon which has become renowned for its superlative properties.<sup>23</sup> For example, pristine graphene has modulus and strength of 1 TPa and 130 GPa respectively.<sup>24</sup> Originally produced in very small quantities,<sup>25</sup> graphene can now be produced in large quantities by exfoliation<sup>26</sup> of graphite in solvents,<sup>27</sup> aqueous surfactant solutions<sup>28</sup> or polymer solutions.<sup>29, 30</sup> Already, graphene has displayed significant success in reinforcing<sup>31-34</sup> both thermoplastics<sup>35-37</sup> and elastomers,<sup>38, 39</sup> in some cases at very low loading level.<sup>36, 40, 41</sup>

With this in mind, graphene appears to be a promising additive for thermoplastic adhesives. However, to the best of our knowledge, no work has been done on this area. In this report, we use solution processing to prepare composites of PVAc and solvent exfoliated graphene. We show that the addition of <1% graphene can result in a doubling of the composite strength and stiffness without significant reduction in ductility. In addition, we find the adhesive properties of the composite to be significantly better than the neat polymer.

## 2. Experimental procedure

Graphite powder (10 g, Sigma Aldrich) was exfoliated by sonicating (GEX600, 24 kHz, flat head probe, 25% amplitude) in 100 ml NMP (100 mg/ml) for 6 h. The resulting dispersion was centrifuged at 1000 rpm for 45 minutes (Hettich Mikro 22R). This results in the sedimentation of unexfoliated graphite and large graphene flakes. The sediment was collected and redispersed in fresh NMP by sonicating in a sonic bath (Branson 1510E-MT) for 15 minutes. This dispersion was centrifuged at 500 rpm for 45 minutes to remove the unexfoliated graphite. The supernatant, which is expected to contain reasonably large graphene flakes,<sup>42</sup> was retained. This supernatant was filtered through a nylon 0.45  $\mu\text{m}$  membrane and washed with 200 ml THF, resulting in a re-aggregated graphene filter cake. Previous studies have shown that such materials tend to be free of defects and oxides and consist of flakes of good quality graphene.<sup>27, 43</sup> In addition, such cakes are known to be easily redispersed in appropriate solvents.<sup>44</sup> During this work, it was found that re-aggregated graphene filter cakes could be effectively redispersed, even in poor solvents such as THF.

Such a dispersion (5mg/ml), prepared by bath sonication (Branson 1510E-MT, for 4 h) was used as a graphene stock dispersion. While such dispersions are unstable, they can be stabilised by subsequent addition of a polymer such as PVAc. If carefully chosen, the polymer can partially bind to the graphene sheets stabilising them against re-aggregation by the steric mechanism.<sup>30</sup> Polyvinyl acetate (Sigma Aldrich,  $M_w=100,000$  g/mol) was dissolved in THF at two concentrations, 30 mg/ml and 200 mg/ml. These solutions were blended with a graphene/THF dispersion (5 mg/ml) in the required ratio to give the desired graphene/PVAc mass fraction. The resulting mixtures were further bath sonicated for 4 h to homogenise. These dispersions were stable with no visible evidence of aggregation in the liquid phase. Dispersions were characterised by depositing a drop of liquid onto a holey carbon TEM grid and analysed using a Jeol 2100.

The composite dispersions with PVAc concentration of 30 mg/ml were poured into Teflon trays and dried at room temperature for 24 h and then at 60 °C for 8 h. They were cut into strips of thickness  $\sim 50$   $\mu\text{m}$  and lateral dimensions 2.5 mm $\times$ 20 mm using a die cutter. Tensile testing was performed with a Zwick Z100 at a strain rate of 15 mm/min. The fracture surfaces were imaged using a Zeiss Ultra SEM operating at 2 kV. The mass fractions were converted to volume fraction assuming mass densities of  $\rho_G=2100$  kg/m<sup>3</sup> and  $\rho_P=1180$  kg/m<sup>3</sup>.

The composite dispersions with PVAc concentration of 200 mg/ml were used for adhesive testing. In all cases, equal masses of the high concentration dispersion were spread on a wood surface over a well-defined area. An identical piece of wood was then pressed onto the glue. These assemblies were then placed in a custom built holder and  $\sim 0.042$  MPa applied for three days at room temperature and further dried over night at 60 °C. Both tensile and shear adhesive testing was performed. For tensile tests the wood pieces were in the shape of the letter T with the glue applied to the top of the T over an area of 2.5 mm  $\times$  27 mm. During testing the applied stress was in a direction perpendicular to the glued surface. For shear tests the wood was in the shape of a bar with the glue applied to the side of the bar over an area of 10 mm  $\times$  14 mm. During testing the applied stress was in a direction parallel to the glued surface. In each case the strain rate was 0.1 mm/min. For both shear and tensile measurements 3-5 assemblies were tested for both polymer and composite adhesives.

### 3. Results and Discussion

High concentration dispersions of graphene in THF (5 mg/ml) were mixed with solutions of PVAc in THF (30 mg/ml) to yield hybrid polymer-graphene dispersions with graphene volume fractions in the range 0% to 0.85%. The exfoliation state of the graphene in these hybrid dispersions can be assessed by TEM. Shown in figure 1A&B are TEM images of typical exfoliated graphene flakes. They appear to be of good quality, with no holes or other obvious defects. It is well known from previous studies that graphene prepared in this way is largely defect free.<sup>43, 45</sup> Image analysis shows the mean flake length and width to be 1.5  $\mu\text{m}$  and 0.7  $\mu\text{m}$  respectively. Flake edge analysis<sup>43</sup> suggests the flakes to contain between 1 and 6 graphene monolayers with a mean of  $\sim 3$ . Thus it is important to note that the dispersions consist predominately of multi-layer graphene.

Shown in figure 1C are free standing films of PVAc and PVAc/graphene composites (volume fractions of 0 to 0.84%). It can be seen that while the dispersion is reasonably good, some aggregation cannot be avoided, even at low volume fractions. This aggregation probably occurs during film drying due to the increasing graphene/THF concentration. Figure 1 D&E show SEM images of the fracture surfaces of PVAc and PVAc/graphene films respectively. While the polymer film shows a relatively featureless surface, the presence of graphene greatly alters the film morphology with numerous graphene sheets observable.

We performed tensile tests on films with a range of mass fractions (figure 2). For the polymer the stress initially increases non-linearly with strain. The polymer yields at approximately 5% strain above which the stress falls off. This behaviour is in line with previous reports of the tensile response of PVAc,<sup>46</sup> although it is important to stress that the mechanical response of PVAc at room temperature is very sensitive to strain rate.<sup>19</sup> The composites stress strain curves show greater linearity at low strain but otherwise have broadly similar shapes to the polymer.

From these stress strain curves, we can obtain a number of mechanical parameters. Shown in figure 3A is the Young's modulus,  $Y$ , plotted as a function of graphene volume fraction. The modulus increases linearly with graphene content from 0.75 GPa for the polymer to 1.5 GPa for the 0.1 vol% composite. The initial rate of increase was  $dY/dV_f=530$  GPa, reasonably close to the maximum value of 1TPa set by the graphene sheet modulus and the rule of mixtures.<sup>24, 47</sup> It is likely that this value is lower than 1 TPa because of the finite length of the flakes used in this study.<sup>36</sup> This result agrees well with the value of 680 GPa measured for graphene/polyvinylalcohol composites.<sup>36</sup> At higher volume fractions the

modulus falls off before rising again albeit at a slower rate. This behaviour may be indicative of aggregation. We note that the initial increase is competitive with published data (expressed in terms of filler mass fraction,  $M_f$ ) for PVAc reinforced with cellulose nanofibers ( $dY/dM_f \approx 80$  GPa)<sup>19</sup>, carbon nanotubes ( $dY/dM_f \approx 200$  GPa)<sup>18</sup> and nanoclays ( $dY/dM_f \approx 340$  GPa)<sup>20</sup>. (NB, the last value was calculated for only two data points so must be treated with caution. The vast majority of clay-polymer composites show much lower reinforcement.<sup>21</sup>)

Very similar behaviour was observed for the ultimate tensile strength,  $\sigma_B$ , which increased linearly from 21 MPa for the polymer to 38 MPa for the 0.1 vol% composite with a slope of  $d\sigma_B/dV_f = 15$  GPa (figure 3B). Such a large increase at such a low loading level is impressive and is generally only found for high performance nano-fillers. For example, this result compares well to the value of  $d\sigma_B/dV_f = 22$  GPa measured for graphene/polyvinylalcohol composites.<sup>36</sup> Again, this value is also similar to published data for PVAc reinforced with carbon nanotubes ( $d\sigma_B/dM_f \approx 10$  GPa)<sup>18</sup> but much higher than equivalent data for cellulose nanofibers ( $d\sigma_B/dM_f \approx 0.2$  GPa)<sup>19</sup>. However, the slope is much less than the value of 130 GPa predicted by the graphene sheet strength and the rule of mixtures.<sup>24, 47</sup> However, this probably means that the flake length is below the critical length<sup>48</sup> (expected to be of order of many microns<sup>29, 49</sup>). Under such circumstances, material fracture generally involves failure of the polymer-graphene interface rather than breaking of the flakes.<sup>5, 36, 48</sup> Under these circumstances, we can write  $d\sigma_B / dV_f \approx \tau_B [\langle L \rangle + \langle w \rangle] / 4 \langle t \rangle$  where  $\tau_B$  is the interfacial strength.<sup>36</sup> Using the flake dimensions given above, this means  $\tau_B \approx 27$  MPa, similar to the value of 29 MPa recently measured for graphene/PVA composites.<sup>36</sup> Indeed, given the structural similarities between PVAc and PVA, it is hardly surprising that their interfaces with graphene have similar shear strength.

We note that both  $dY/dV_f$  and  $d\sigma_B/dV_f$  values we have measured for PVAc-graphene composites are quite high as discussed above. That the value of  $dY/dV_f$  is high implies that the polymer-graphene interfacial stress-transfer is very effective while the relatively large value of  $d\sigma_B/dV_f$  implies a strong polymer-graphene interface. Taken together this suggests a strong interaction between PVAc and graphene. As described above, a similarly strong interaction is observed for PVA-graphene composites.<sup>36</sup> The detailed nature of these interactions is not well understood. However, we suggest that the results described above are consistent with the hydrogenated parts of the polymer chain binding strongly to the graphene by dispersive interactions. It is likely that the polar acetate group (or hydroxyl group in the

case of PVA) protrudes outward and so is available to interact with other polymer chains. However, molecular dynamics simulations are required to test this hypothesis.

The strain at break appeared to increase slightly from ~100% for the polymer to ~175% for the 0.23vol% composite sample before subsequently falling off. This is slightly unusual as ductile polymers usually display a decrease on strain at break on the addition of nano-fillers such as nanotubes or graphene.<sup>39, 50-52</sup> Indeed previous work on PVAc filled with nanotubes or nanoclays showed a reduction in ductility for all filler contents.<sup>18, 19</sup> It is not clear why this should be the case. However, for polymers which fail by craze formation, if the fibular bridges were reinforced by the presence of the nano-filler, this might result in an increase in ductility in the composite.

Because one of the most common applications of PVAc is as an adhesive,<sup>10, 13, 14</sup> we tested the effect of adding graphene on the adhesive properties of PVAc. We prepared very high concentration solutions of PVAc in THF (200 mg/ml) both with and without the presence of various amounts of graphene from 0.2wt% to 3wt%. These viscous liquids were then coated on pieces of wood over a well-defined area as an adhesive. Identical pieces of wood were then pressed onto the adhesive in geometries designed to test both the tensile and shear properties of the adhesive (Figure 4A). The glued assemblies were then pulled apart using a tensile tester (figure 4B). Typical stress-strain curves for polymer and composite adhesives, tested in both tensile and shear geometries are shown in figure 4C. For both shear and tensile measurements, the stress strain curve looked very different to the tensile stress strain curves of the PVAc and PVAc/graphene composites shown in figure 2. Indeed this suggests that the mechanical properties of the bond are not controlled solely by the mechanical properties of the adhesive.

The tensile adhesive strength increased sublinearly from 0.3 MPa for the pure polymer to 0.75 MPa for the 3wt% composite. The shear strength increased linearly from 0.5 MPa for the PVAc to 2.2 MPa for the 4wt% sample. Interestingly the initial rate of increase of both shear and tensile adhesive strength is similar at ~50 MPa. This is considerable lower than the rate of increase of composite tensile strength with graphene mass fraction again indicating that the bond strength is not solely limited by the strength of the composite. This suggests that failure may be adhesive rather than cohesive. We can compare this with Kaboorani et al<sup>10</sup> who tested PVAc filled with 4% nanoclay. They achieved 25% increase in

adhesive strength, albeit from a much higher base (the shear strength of their commercial PVAc adhesive was ~19 MPa).

We also measured the area under the stress-displacement curve for each test. This parameter is equal to the energy cost per unit area of breaking the bond between the wood pieces and can be considered the adhesive toughness. This data is shown in figure 4E. For both tensile and shear tests, the toughness increases dramatically with graphene addition up to 1.5wt% with some falloff observed for the tensile case at higher graphene content. However, the tensile adhesive toughness increased by more than threefold for 0.7wt% graphene addition while the shear toughness had increased by almost fourfold for the 3wt% sample. This is an important result as it shows that graphene-containing adhesives can absorb significantly more energy before failure than the polymer adhesive alone.

We note that the adhesive strength in both tensile and shear modes was less than 3 MPa. Commercially available PVAc glues can have strengths of up to 7 MPa for a range of woods.<sup>4, 13, 14</sup> However, such glues tend to be complex mixtures of PVAc and a range of additives, which have been developed over decades. In comparison, our PVAc adhesives were deposited from simple PVAc solutions. It is important to assess the efficacy of graphene addition to commercially available PVAc wood glue. To test this, we purchased Tonic Studio Craft Glue PVAc wood glue. The concentration of solids (mainly PVAc) in the glue was measured by drying a known volume of glue (1ml) at 60C for three days to remove the solvent (water) followed by weighing. The commercial glue was then mixed with a 5mg/ml Graphene/THF stock solution. Excess solvent was evaporated to bring the glue back to its original concentration (although now dissolved in a THF/water mixture rather than purewater). Shear and tensile tests were carried out as before both on samples bonded with as-purchased glue and those bonded with commercial glue with graphene added (during the graphene addition process, one sample was prepared with processing identical to the composites but with no added graphene. This sample is included in the composite glue data set but with graphene content = 0). Representative stress-displacement curves are shown in figure 4F and were found to be considerably different to those measured before, possibly due to the presence of additives in the commercial glue. We found no significant improvement in the adhesive shear strength on addition of graphene. However, small but significant changes were observed for the tensile adhesive strength. On addition of graphene, the tensile adhesive strength increased linearly from 1.25 MPa for the glue reference sample to 1.75 MPa for the sample containing 0.7 wt% graphene before falling off at higher loading levels. Importantly,

we found that the dilution/re-concentration procedure used to add the graphene had no effect on the tensile adhesive strength of the graphene-free glue; identical values were found for the pristine PVAc glue and PVAc glue that had been treated identically to the composites but with no graphene added. This shows that graphene addition can have a positive effect on commercial PVAc glue.

We also calculated the adhesive toughness for all glues based on the commercial adhesive. This data is shown in figure 4H. Increases in both tensile and shear toughness were observed. The tensile adhesive toughness increased from  $0.2 \text{ kJ/m}^2$  for the as-purchased glue to  $1.5 \text{ kJ/m}^2$  for the 0.7 wt% sample, a >7-fold increase. It is worth noting that this increase in toughness is mostly due to increases in displacement at failure (see figure 4B) on addition of graphene. A much smaller but still significant increase in the shear toughness was observed.

It is worth considering the mechanism of failure. Under stress, it is known that cavities begin to form in the adhesive.<sup>11</sup> When failure is cohesive these cavities tend to be wholly contained within the adhesive. Cavity formation tends to first occur close to the yield stress (i.e. the maximum stress observed in the stress strain curves in figures 3 and 4B).<sup>11</sup> Once the cavities have formed, the stress is maintained by fibrils in a manner similar to crazing in polymers.<sup>5</sup> As the displacement is increased the cavities expand and the fibrils become extended. This process dissipates considerable amounts of energy, often resulting in high adhesive toughness. Failure occurs when the last fibril breaks. Such fibrils can be observed in figure 4B just before failure. The addition of graphene results in increases in adhesive stress because graphene both stiffens and strengthens the polymer resulting in cavity formation at higher stress and the fibrils resisting deformation with greater stress. The increased work of adhesion is largely due to failure occurring at higher displacements and is due to the reinforcement of the fibrils which delays failure to higher displacements.

#### 4. Conclusion

In conclusion, we have shown that the polymer PVAc can be mechanically reinforced by addition of solvent exfoliated graphene. Addition of ~0.1 vol% graphene results in the doubling of modulus, strength and ductility. When used as an adhesive addition of 0.7% graphene results in increases in both adhesive strength and toughness. We believe graphene shows great promise as an additive for adhesives. It is produced from a precursor, graphite, which is very cheap making it economically plausible. In addition, the results presented here

represent only the first tentative steps in this area. Further work is likely to see further advances in both strength and toughness of graphene reinforced adhesives.

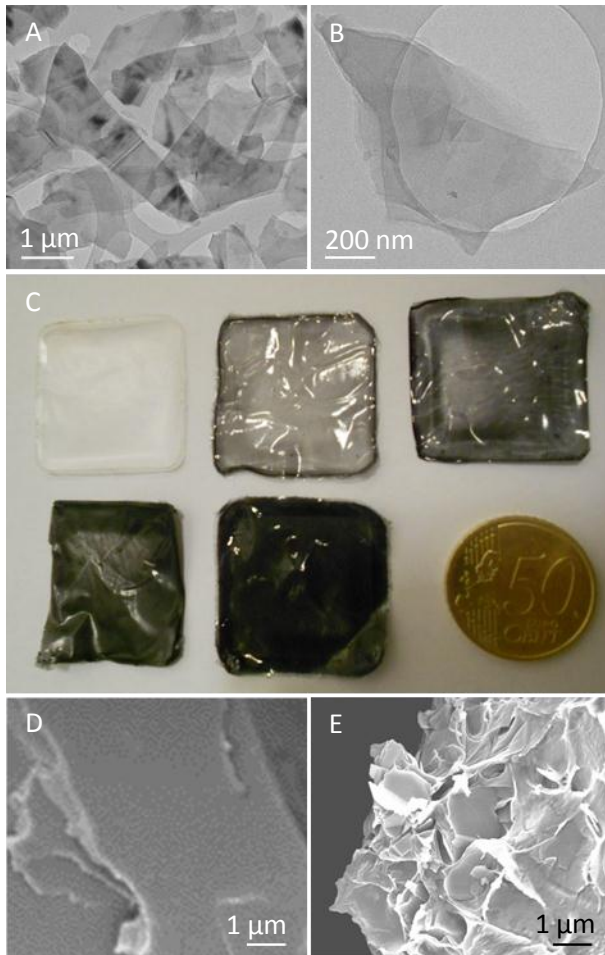


Figure 1: A) Large numbers of multilayer graphene deposited on a holey carbon TEM grid. B) An individual graphene multilayer. C) Photograph of PVAc-graphene films with mass fractions of 0%, 0.2%, 0.4%, 0.7% 1.5% (volume fractions from 0% to 0.8%). SEM image of D) a PVAc and E) a PVAc/graphene fracture surface.

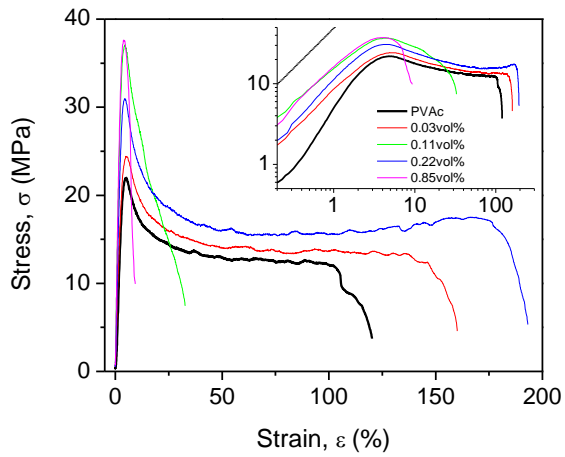


Figure 2: Stress strain curves for the PVAc/graphene composite film studied in this work. Inset: Stress-strain curves on a log-log scale. The dotted line represents linearity.

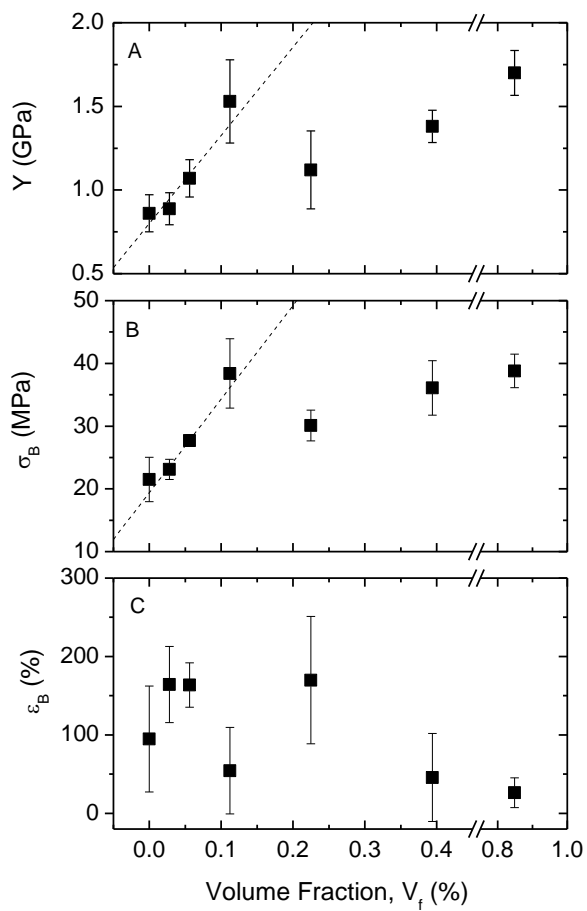


Figure 3: Mechanical properties of PVAc films; A) Young's modulus, B) ultimate tensile strength and C) strain at break, as a function of graphene volume fraction.

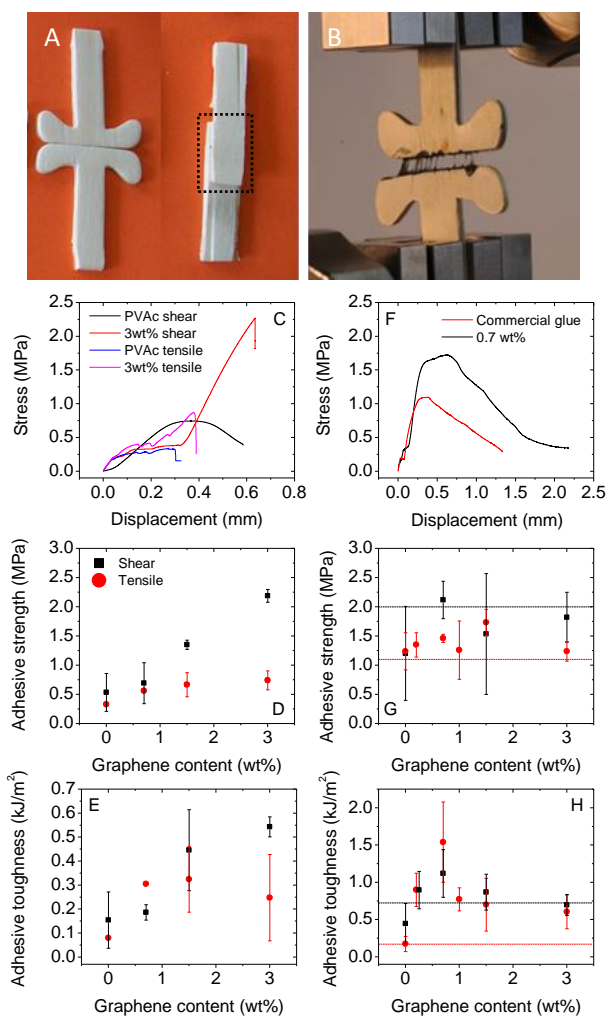


Figure 4: Measurements of adhesive properties of PVAc/graphene glue. A) Photograph of samples used for adhesive testing. Left: Two T-shaped wood pieces glued together for tensile testing. Right: Two wooden bars, glued together along an overlapping region (dashed line), for use in shear measurements. B) Photograph of T-shaped pieces during a tensile test. C) The applied stress is plotted as a function of displacement in both tensile and shear modes for samples glued using home-made PVAc adhesive. D-E) Tensile and shear bond strength (D) and toughness (E) as a function of graphene content for the home-made PVAc adhesives. F) Tensile stress-strain curves for as-bought commercially available glue and same with 0.7wt% graphene added. G-H) Tensile and shear bond strength (G) and toughness (H) as a function of graphene content for the adhesives prepared with commercially available PVAc glue. The dotted lines represents the untreated glue. The data points represent the glue, diluted and re-concentrated during the process of graphene addition.

## Acknowledgements

We acknowledge financial support from Science Foundation Ireland through the Principle Investigator scheme (grant number 07/IN.7/I1772).

## References

- (1) Yacobi, B. G.; Martin, S.; Davis, K.; Hudson, A.; Hubert, M., *J. Appl. Phys.* **2002**, *91*, 6227-6262.
- (2) Gegner, J., *Materialwiss. Werkstofftech.* **2008**, *39*, 33-44.
- (3) Park, S. Y.; Choi, W. J.; Choi, H. S.; Kwon, H.; Kim, S. H., *J. Adhes.* **2010**, *86*, 192-221.
- (4) Hatano, Y.; Tomita, B.; Mizumachi, H., *Holzforschung* **1986**, *40*, 255-258.
- (5) Callister, W. D., *Materials Science and Engineering an Introduction*. 7th ed.; Wiley: 2007; p 721.
- (6) Lim, W. W.; Mizumachi, H., *J. Appl. Polym. Sci.* **1997**, *66*, 525-536.
- (7) Pastor-Sempere, N.; Fernandez-Garcia, J. C.; Orgiles-Barcelo, A. C.; Sanchez-Adsuar, M. S.; Martin-Martinez, J. M., *J. Adhes.* **1996**, *59*, 225-239.
- (8) Torro-Palau, A.; Fernandez-Garcia, J. C.; Orgiles-Barcelo, A. C.; Martin-Martinez, J. M., *J. Adhes.* **1996**, *57*, 203-225.
- (9) Zhai, L. L.; Ling, G. P.; Li, J.; Wang, Y. W., *Mater. Lett.* **2006**, *60*, 3031-3033.
- (10) Kaboorani, A.; Riedl, B., *Composites Part A* **2011**, *42*, 1031-1039.
- (11) Wang, T.; Lei, C. H.; Dalton, A. B.; Creton, C.; Lin, Y.; Fernando, K. A. S.; Sun, Y. P.; Manea, M.; Asua, J. M.; Keddie, J. L., *Adv. Mater.* **2006**, *18*, 2730-2734.
- (12) Gilbert, E. N.; Hayes, B. S.; Seferis, J. C., *Polym. Eng. Sci.* **2003**, *43*, 1096-1104.
- (13) Burdurlu, E.; Kilic, Y.; Eli'bol, G. C.; Kilic, M., *J. Appl. Polym. Sci.* **2006**, *100*, 4856-4867.
- (14) Dajbych, O.; Herák, D.; Sedláček, A.; Gürdil, G., *Res. Agric. Eng.* **2010**, *56*, 159-165.

- (15) Dalton, A. B.; Collins, S.; Munoz, E.; Razal, J. M.; Ebron, V. H.; Ferraris, J. P.; Coleman, J. N.; Kim, B. G.; Baughman, R. H., *Nature* **2003**, *423*, 703-703.
- (16) Vigolo, B.; Penicaud, A.; Coulon, C.; Sauder, C.; Pailler, R.; Journet, C.; Bernier, P.; Poulin, P., *Science* **2000**, *290*, 1331-1334.
- (17) Coleman, J. N.; Khan, U.; Blau, W. J.; Gun'ko, Y. K., *Carbon* **2006**, *44*, 1624-1652.
- (18) Maksimov, R. D.; Biteniekis, J.; Plume, E.; Zicans, J.; Meri, R. M., *Mech. Compos. Mater.* **2010**, *46*, 237-250.
- (19) Gong, G.; Pyo, J.; Mathew, A. P.; Oksman, K., *Composites Part A* **2011**, *42*, 1275-1282.
- (20) Mansoori, Y.; Akhtarparast, A.; Zamanloo, M. R.; Imanzadeh, G.; Masooleh, T. M., *Polym. Compos.* **2011**, *32*, 1225-1234.
- (21) Pavlidou, S.; Papaspyrides, C. D., *Prog. Polym. Sci.* **2008**, *33*, 1119-1198.
- (22) Zhu, L. J.; Narh, K. A., *J. Polym. Sci., Part B: Polym. Phys.* **2004**, *42*, 2391-2406.
- (23) Geim, A. K., *Science* **2009**, *324*, 1530-1534.
- (24) Lee, C.; Wei, X. D.; Kysar, J. W.; Hone, J., *Science* **2008**, *321*, 385-388.
- (25) Novoselov, K. S.; Jiang, D.; Schedin, F.; Booth, T. J.; Khotkevich, V. V.; Morozov, S. V.; Geim, A. K., *Proc. Natl. Acad. Sci. U. S. A.* **2005**, *102*, 10451-10453.
- (26) Coleman, J. N., *Acc. Chem. Res.* **2013**, *46*, 14-22.
- (27) Hernandez, Y.; Nicolosi, V.; Lotya, M.; Blighe, F. M.; Sun, Z. Y.; De, S.; McGovern, I. T.; Holland, B.; Byrne, M.; Gun'ko, Y. K.; Boland, J. J.; Niraj, P.; Duesberg, G.; Krishnamurthy, S.; Goodhue, R.; Hutchison, J.; Scardaci, V.; Ferrari, A. C.; Coleman, J. N., *Nat. Nanotechnol.* **2008**, *3*, 563-568.
- (28) Lotya, M.; Hernandez, Y.; King, P. J.; Smith, R. J.; Nicolosi, V.; Karlsson, L. S.; Blighe, F. M.; De, S.; Wang, Z. M.; McGovern, I. T.; Duesberg, G. S.; Coleman, J. N., *J. Am. Chem. Soc.* **2009**, *131*, 3611-3620.
- (29) Khan, U.; May, P.; O'Neill, A.; Bell, A. P.; Boussac, E.; Martin, A.; Semple, J.; Coleman, J. N., *Nanoscale* **2012**, *5*, 581-7.
- (30) May, P.; Khan, U.; Hughes, J. M.; Coleman, J. N., *J. Phys. Chem. C* **2012**, *116*, 11393-11400.
- (31) Kim, H.; Abdala, A. A.; Macosko, C. W., *Macromolecules* **2010**, *43*, 6515-6530.

- (32) Kuilla, T.; Bhadra, S.; Yao, D. H.; Kim, N. H.; Bose, S.; Lee, J. H., *Prog. Polym. Sci.* **2010**, *35*, 1350-1375.
- (33) Young, R. J.; Kinloch, I. A.; Gong, L.; Novoselov, K. S., *Compos. Sci. Technol.* **2012**, *72*, 1459-1476.
- (34) Potts, J. R.; Dreyer, D. R.; Bielawski, C. W.; Ruoff, R. S., *Polymer* **2011**, *52*, 5-25.
- (35) Khan, U.; Young, K.; O'Neill, A.; Coleman, J. N., *J. Mater. Chem.* **2012**, *22*, 12907-12914.
- (36) May, P.; Khan, U.; O'Neill, A.; Coleman, J. N., *J. Mater. Chem.* **2011**, *22*, 1278-1282.
- (37) Ramanathan, T.; Abdala, A. A.; Stankovich, S.; Dikin, D. A.; Herrera-Alonso, M.; Piner, R. D.; Adamson, D. H.; Schniepp, H. C.; Chen, X.; Ruoff, R. S.; Nguyen, S. T.; Aksay, I. A.; Prud'homme, R. K.; Brinson, L. C., *Nat. Nanotechnol.* **2008**, *3*, 327-331.
- (38) Menes, O.; Cano, M.; Benedito, A.; Gimenez, E.; Castell, P.; Maser, W. K.; Benito, A. M., *Compos. Sci. Technol.* **2012**, *72*, 1595-1601.
- (39) Khan, U.; May, P.; O'Neill, A.; Coleman, J. N., *Carbon* **2010**, *48*, 4035-4041.
- (40) Rafiee, M. A.; Rafiee, J.; Wang, Z.; Song, H. H.; Yu, Z. Z.; Koratkar, N., *Acs Nano* **2009**, *3*, 3884-3890.
- (41) Morimune, S.; Nishino, T.; Goto, T., *Polym. J.* **2012**, *44*, 1056-1063.
- (42) Khan, U.; O'Neill, A.; Porwal, H.; May, P.; Nawaz, K.; Coleman, J. N., *Carbon* **2010**, *50*, 470-475.
- (43) Khan, U.; O'Neill, A.; Lotya, M.; De, S.; Coleman, J. N., *Small* **2010**, *6*, 864-871.
- (44) Khan, U.; Porwal, H.; O'Neill, A.; Nawaz, K.; May, P.; Coleman, J. N., *Langmuir* **2011**, *27*, 9077-9082.
- (45) O'Neill, A.; Khan, U.; Nirmalraj, P. N.; Boland, J. J.; Coleman, J. N., *J. Phys. Chem. C* **2011**, *115*, 5422-5428.
- (46) Ochigbo, S. S.; Luyt, A. S.; Focke, W. W., *J. Mater. Sci.* **2009**, *44*, 3248-3254.
- (47) Padawer, G. E.; Beecher, N., *Polym. Eng. Sci.* **1970**, *10*, 185-192.
- (48) Hull, D.; Clyne, T. W., *An Introduction to Composite Materials*. Cambridge University Press: New York, 1996; p 344.

- (49) Gong, L.; Kinloch, I. A.; Young, R. J.; Riaz, I.; Jalil, R.; Novoselov, K. S., *Adv. Mater.* **2010**, *22*, 2694-2697.
- (50) Blighe, F. M.; Blau, W. J.; Coleman, J. N., *Nanotechnology* **2008**, *19*, 415709.
- (51) Khan, U.; Blighe, F. M.; Coleman, J. N., *J. Phys. Chem. C* **2010**, *114*, 11401-11408.
- (52) Khan, U.; May, P.; O'Neill, A.; Vilatela, J. J.; Windle, A. H.; Coleman, J. N., *Small* **2011**, *7*, 1579-1586.

## ToC graphic

